WOOD RESEARCH doi.org/10.37763/wr.1336-4561/69.3.485494
e-ISSN 2729-8906
69(3): 2024 485-494 pp.

DETERMINATION OF FLEXURAL STRENGTH AND YOUNG'S MODULUS OF ELASTICITY OF ACTIVELY BENT WOOD

ROMAN HERDA, MILOŠ SLIVANSKÝ, JÁN BRODNIANSKY, TOMÁŠ KLAS
SLOVAK UNIVERSITY OF TECHNOLOGY IN BRATISLAVA
SLOVAK REPUBLIC

(RECEIVED JULY 2024)

ABSTRACT

The article focuses on the experimental verification of wooden laths with a cross-section of 10 mm x 40 mm which were selected for active bending. The laths are made of pine wood and are 2 m in length. The research includes experimental measurements to determine the limit deformations achieved by bending the wood without chemical treatment, by applying compressive force to an originally straight beam, causing it to buckle and further deform. Ten bending tests of beams were performed, and from the same pieces, 21 tests were conducted using the four-point bending test to determine the flexural strength, and 30 tests to determine the global modulus of elasticity.

KEYWORDS: Active bending, flexural strength, modulus of elasticity, wood.

INTRODUCTION

Active bending of wood represents a complex issue that is extensively utilized in the furniture industry (Zemiar 2007). However, it also poses a challenging engineering task in construction, where it is necessary to achieve the shape of a structure with significant geometric curvature.

In construction, active bending of wood opens new possibilities for creating aesthetically appealing and functional building structures, thereby contributing to the development of sustainable architecture. Notable structures with curved shapes built using timber and the method of active bending during the construction process include: the pool roof in Saint-Quentin-en-Yvelines in France (D´Amico 2015), the Multihalle in Mannheim (Liddel 2015), and the Weald and Downland construction (Collins 2016).

Active bending can be defined as a systematic elastic deformation, where the resulting geometry of the structure is achieved by transforming from an initial unstressed geometry to the resulting curved geometry with stress in the load-bearing elements. Integrating active bending of wood into the construction process to create the desired curved geometry allows the full potential of wood as a building material to be utilized. Wood is a material with suitable properties, which include not only flexibility and strength but also the ability to maintain its shape after bending. The ability to elastically transform the material depends on the ratio of bending strength to Young's modulus of elasticity (Ashby 2004). The main disadvantage of active bending of wood is the residual stress that is introduced into the rods during the assembly stage. Today, shapes with large spans and small radii of curvature are preferred. Gengnagel et al. (2013) described that to achieve the smallest possible radius of curvature, it is necessary to achieve a low ratio of the modulus of elasticity to bending strength.

There are several ways to ensure the resulting shape of the structure with curved geometry. The most commonly used deformation methods in practice, described by Quinn et al. (2015), include bending by lifting, pushing, lowering, and inflating using pneumatic cushions (Quinn 2018). The deformation method that is the subject of the study in this article focuses on the deformation of beams due to compressive loading, which in the first step causes buckling of the beam upon reaching the critical force Ncr (N) and with subsequent additional loading of the beam with deformation, there is an increase in vertical and horizontal deformation (Fig. 1). Research on this type of loading has been conducted by Gengnagel et al. (2014), Cuvilliers (2014), Mesnil (2013).

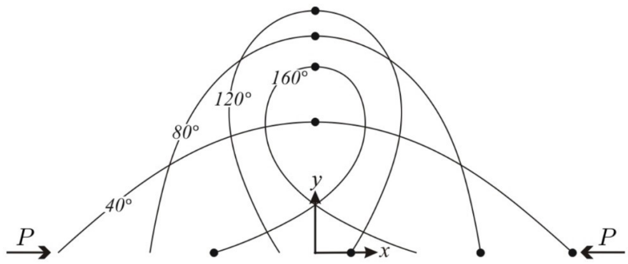

Fig. 1: Deformation curves of the beam caused by axial force (D´Amico et al. 2016).

Based on the aforementioned properties of wood associated with active bending, this article focuses on bending tests of visually sorted beams with dimensions of 40 x 10 x 2000 mm to determine the limit stress values at the failure of the bent sample subjected to horizontal loading, as well as the limit horizontal and vertical deformation. Given that the ability of the material to actively bend depends on an appropriate ratio of Young's modulus of elasticity (Ravenshort et al. 2014, Aicher et al. 2002, Purba 2019) and bending strength (Lienhard et al. 2013, Collins et al. 2015), tests were conducted to determine these two parameters using a four-point bending test prepared according to EN 408 (2005). The principles of experimental measurement are based on the findings of previously conducted research on the topic of active bending (Colabella et al. 2015, Bocanegra et al. 2020, Bocanegra et al. 2022, Damico and Zhang 2014, Cichocka 2020).

MATERIAL AND METHODS

For the experimental measurements, a set of wooden slats with a cross-section of 10 mm x 40 mm and a length of 2000 mm was used. The samples were tested to determine the maximum deformations and stresses during active bending before the beam failed (Fig. 2). Bending tests of the entire beams were performed, and subsequently, material tests were conducted to determine the Young's modulus of elasticity in bending and the bending strength. A S9M force gauge with an accuracy class of 0.02 and a range of up to 50 kN was used to measure the magnitude of the applied force. Inductive displacement sensors WA with a range of 0-500 mm were used to measure the magnitude of the deformations. When the deformation value exceeded 500 mm, for large arch deflections, the measurement continued by connecting a new inductive measuring device. The moisture content of the tested samples was between 9% and 10%.

Preparation of samples and testing setup for active bending

The loading scheme includes a simply supported beam, where the application of compressive force to the initially straight beam causes it to buckle (Fig. 2). Before the beam buckles, the main acting component of the internal forces is the axial compressive force. After the beam buckles, loading continues, and due to the change in the geometry and shape of the beam, a significant bending moment arises in addition to the axial force. The aim of the loading is to determine the maximum vertical and horizontal deformation and bending strength of the tested wooden samples before failure.

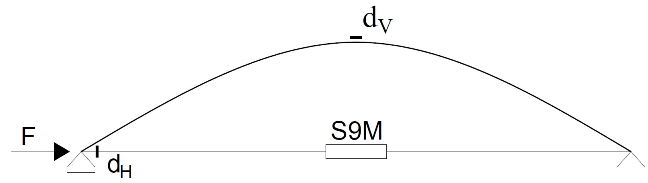

Fig. 2: The load scheme and the scheme of the measurement devices.

In accordance with the load scheme (Fig. 2), a loading assembly (Fig. 3) was created, respecting the loading method and boundary conditions.

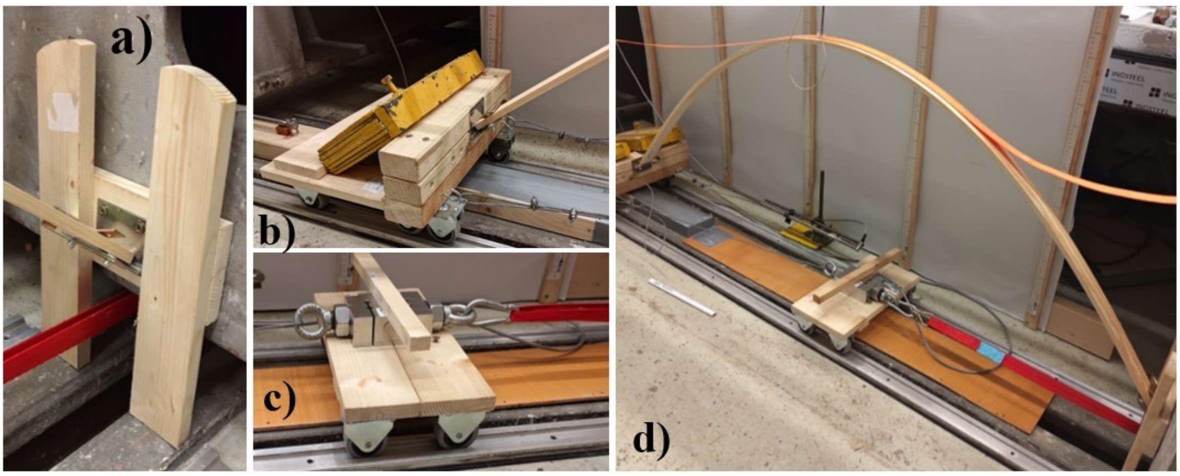

Fig. 3: a) Fixed hinge support, b) sliding hinge support, c) measurement device S9M, d) loading assembly during testing.

On the left side, there is a sliding hinge support, and on the right side, a fixed hinge support. The displacement sensors were positioned at points to measure vertical deformation and horizontal displacement. To ensure the buckling shape, an initial imperfection of 20 mm was applied to the center of the wooden beam.

Determining the flexural strength and Young's modulus of elasticity in bending

To determine the flexural strength and global modulus of elasticity, a four-point bending test was used (Fig. 4). The dimensions of the samples were adjusted according to the requirements of EN 408 (2005). The length of the samples was 200 mm. The cross-sectional dimensions of each sample were measured with an accuracy of 0.01 mm and recorded in the report.

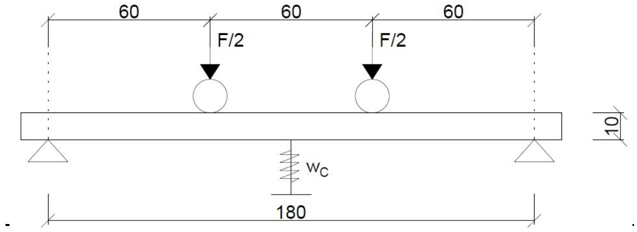

Fig. 4: Assembly scheme for the four-point bending test.

The test assembly for determining the flexural strength of wood was constructed in accordance with the EN 408 (2005). Given the thickness of the tested wooden specimens with a value of □ representing 10 mm, the distance between the supports was set to 18 h. The load was applied symmetrically to the test assembly at a distance of 6 h from the supports. The magnitude of the vertical deformation was measured at the lower tensile edge in the center of the span between the supports.

The values of the global modulus of elasticity are expressed according to:

$$E_{m,g} = \frac{l^3(F_2 - F_1)}{bh^3(w_2 - w_1)}\left[\left(\frac{3a}{4l}\right) - \left(\frac{a}{l}\right)^3\right] \quad (1)$$

where: $E_{m,g}$ - the global modulus of elasticity (GPa), l - the distance between the support points (mm), a - the distance between the load application point and the nearest support (mm), $F_2 - F_1$ - the increment of load on the linear part of the load-deformation curve (N), $w_2 - w_1$- the increment of deformation corresponding to $F_2 - F_1$ (mm).

In determining the value of the global modulus of elasticity, the sample was tested under a constant loading rate. The displacement rate of the applied load was set according to EN 408 (2005) at 0.03 mm/s, with the maximum load not exceeding 0.4*Fmax. The values of bending strength are expressed according to the following relationship:

$$f_m = (a \cdot F_{max})/(2W) \quad (2)$$

where: f_m - the bending strength (MPa), W - the section modulus (mm^3).

In determining the bending strength, a constant loading rate was defined so that the maximum load was reached within 300 ± 120 s. To determine the value of Fmax and the loading rate, 10 calibration measurements were performed.

RESULTS AND DISCUSSION

Active bending of wooden beams

Experimental bending of wooden beams was conducted on 10 samples labeled L01-L10. During the measurements, the magnitude of the applied force was recorded over time, and the maximum achieved values of vertical and horizontal deformation were monitored. Based on this data, it was possible to determine the stress values at deflection and failure for each sample.

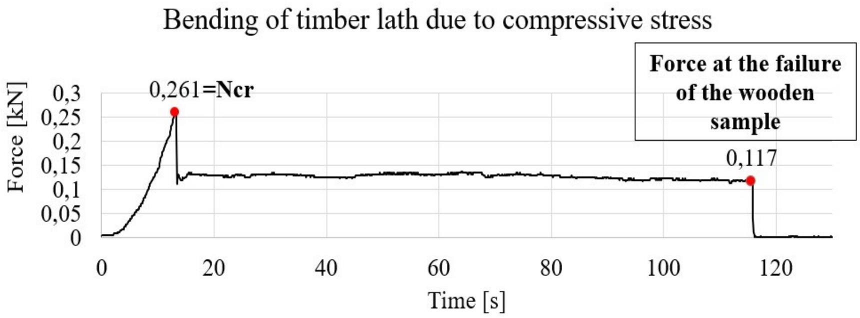

Fig. 5: Graphical dependence of force and time during the loading of sample L01.

The results (Fig. 5) indicate that the maximum force during the loading of sample L01 occurs at the moment when the critical force Ncr (0.261 kN) is reached. At this point, the sample experiences buckling due to compressive stress. Upon applying additional load after buckling, significant deformations occur at a load value lower than the critical force. After reaching the ultimate strength of the tested sample L01, it failed at a force of 0.117 kN and a deflection of 334 mm (Fig. 6).

Fig. 6: Failure of sample L01.

The measurement results (Tab. 1) are divided for each sample from L01 to L10. The measurements recorded the maximum achieved horizontal and vertical deformations and the forces at which buckling and material failure occurred. The loading was applied to the test setup at a constant rate.

Tab. 1: Results of active bending of wooden beams.

	Stress at buckling	Stress at failure	Force at buckling	Force at failure	Vertical deformation at buckling	Maximum vertical deformation	Maximum horizontal deformation
	[MPa]	[MPa]	[kN]	[kN	[mm]	[mm]	[mm]
L01	0.653	93.60	0.261	0.12 0	130	520.0	334.6
L02	0.623	94.82	0.249	0.093	85	679.7	657.9
L03	0.345	107.89	0.138	0.111	61	648.0	610.0
L04	1.163	95.49	0.465	0.099	199	643.0	581.0
L05	0.915	102.32	0.366	0.099	152	689.0	665.0
L06	0.525	110.25	0.210	0.105	85	700.0	676.6
L07	0.735	105.79	0.294	0.108	129	653.0	569.9
L08	1.065	91.65	0.426	0.102	155	599.0	485.0
L09	0.780	107.89	0.312	0.105	116	685.0	604.0
L10	0.548	121.50	0.219	0.120	69	675.0	612.0

The samples were visually sorted to minimize defects in the wooden beams. Despite using the same type of pine wood with identical dimensions, it is not possible to completely eliminate the effects of inhomogeneous between individual samples. This includes not only differences in the structure and orientation of the fibers but also the influence of initial imperfections.

Determination of the global modulus of elasticity and bending strength

The determination of the global modulus of elasticity or wood was carried out in accordance with the EN 408 (2005). To ensure accurate results, the first step involved 11 measurements of calibration test specimens to determine the maximum force at failure and to set the loading rate so that failure occurred within 300 ± 120 s.

Tab. 2: Values of forces and stresses at failure of calibration samples.

	K1	K2	K3	K4	K5	K6	K7	K8	K9	K10	K11
Fmax [kN]	1.731	1.725	1.761	1.959	1.641	1.875	1.884	1.731	1.761	1.629	1.578
fm [MPa]	81.45	81.13	84.37	92.51	78.07	88.30	92.22	85.79	85.99	79.88	74.71

Based on the results from Tab. 2, the average load Fmax at failure of the samples was determined to be 1.752 kN. The determination of the global modulus of elasticity for wood continued with the testing of samples L01-L10. Three measurements were performed on each sample. The result of the measurement is a graphical dependence of force and vertical deformation measured at the center of the span at the point of application of the load. The displacement rate of the applied load was 0.03 mm/s. The resulting measurement values up to 0.4^{*}Fmax were used for regression analysis (Douglas et al. 2012, Akyüz et al. 2019) (Fig. 7).

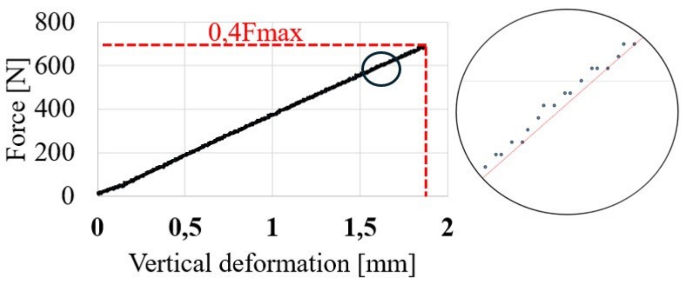

Fig. 7: Graphical representation of results for samples L01-L10 up to 0.4^{*}Fmax.

EN 408 (2005) specifies that, in determining the global modulus of elasticity for wood, the value of the square of the correlation coefficient in the regression analysis should be greater than 0.99. Tab. 3 presents the resulting values for the beams L01-L10.

Tab. 3: Values of the squared correlation coefficients for individual measurements.

	L01	L02	L03	L04	L05	L06	L07	L08	L09	L10
R^2	0.9997	0.9965	0.9998	0.9995	0.9980	0.9997	0.9999	0.997	0.9999	0.9999

Based on the results from the regression analysis presented in Tab. 3, it can be concluded that the mutual dependence between the measured variables is sufficient, and the results are relevant for interpreting the global modulus of elasticity. The resulting values of the moduli of elasticity calculated according to Eq. 1 and the bending strengths calculated according to Eq. 2, along with the ratio of bending strength to Young's modulus, are presented in Tab. 4.

Tab. 4: Resulting values of bending strengths and Young's moduli of elasticity.

	Density	$W_{c,max}$	F_{max}	f_m	$E_{m.g}$	Ratio $f_m/E_{m.g}$
	[kg/m^3]	[mm]	[N]	[MPa]	[GPa]	[-]
L01	487.7	11.9625	1617	79.884	13.104	6.10
					13.974	5.72
					13.061	6.12
L02	721.1	15.35625	2685	125.474	18.113	6.93
					19.051	6.59
					17.812	7.04
L03	638.1	15.5625	2130	97.084	8.423	11.53
					8.692	11.17
					8.566	11.33
L04	542.8	9.13125	1770	85.508	14.139	6.05
					14.402	5.94
					14.003	6.11
L05	533.4	11.478125	1959	92.244	13.571	6.80
					14.034	6.57
					14.003	6.59
L06	641.6	10.790625	2217	103.879	14.036	7.40
					14.089	7.37
					13.673	7.60
L07	605.8	8.459375	1668	81.070	10.995	7.37
					11.058	7.33
					10.665	7.60
L08	543.8	9.1375	1755	82.293	12.402	6.64
					12.361	6.66
					12.118	6.79
L09	576.3	14.396875	2058	99.059	16.315	6.07
					16.526	5.99
					16.044	6.17
L10	678.8	8.596875	2220	105.600	15.216	6.94
					15.402	6.86
					14.685	7.19

According to Ashby's diagram (Ashby 2005), materials are suitable for active bending when the ratio of bending strength to Young's modulus is greater than 2.5.

CONCLUSIONS

This article presents an experimental verification of pine wood beams with a cross-section of 10 mm x 40 mm. The experimental measurement involved bending ten beams of 2 m in length, using compressive loading. Due to the application of compressive stress on originally straight beams, buckling occurs, and with a constant loading rate, further deformation increases. The limit vertical deformations before failure of the samples ranged from 520 mm to 700 mm. Given that the material's ability to deform elastically depends on the ratio of bending strength to Young's modulus, material tests were subsequently performed on samples L01 to L10 to determine these two parameters. To obtain Young's modulus, 30 tests were conducted, with values for individual samples ranging from 8 to 19 GPa. For bending strength determination, 21 four-point bending tests were performed, with resulting values ranging from 79 MPa to 125 MPa. The goal of the experimental measurements was to assess the suitability of the tested material for active bending. Materials suitable for active bending must have a ratio of bending strength to Young's modulus greater than 2.5. Experimental measurements yielded ratios for the individual samples ranging from 5.72 to 11.53, indicating that they can be characterized as suitable for active bending.

ACKNOWLEDGMENTS

This article was created thanks to the support of the scientific grant agency of the Ministry of Education, Science, Research and Sport of the Slovak Republic and the Slovak Academy of Sciences VEGA 1/0397/22. The project could also be created thanks to internal grant of SvF STU, the program for motivation and support for increasing the quality and efficiency of the scientific and research activity of young scientific and research workers 2023.

REFERENCES

1. AICHER. S., HÖFFLIN, L. & BEHRENS, W. (2002): Determination of local and global modulus of elasticity in wooden boards. In: Otto-Graf Journal 13, 16 pp.
2. AKYUZ, I., ERSEN, N., TIRYAKI, S., CAGRI BAYRAM, B., CEMIL AKYUZ, K. & PEKER, H. (2019): Modeling and comparison of bonding strength of impregnated wood material by using different methods: Artificial neural network and multiple linear regression. In: Wood Research 64 (3), ISSN 1336-4561, VUPC (SDVU), 483-498 pp.
3. Ashby, M.F. (2005): Materials selection in mechanical design, Pergamon Press: London, ISBN 0 7506 6168 2, London, 662 pp.
4. BOCANEGRA, A. J. L., MAJANO, A., ARRIAGA, F., GUAITA, M. (2020): Eucalyptus globulus finger jointed solid timber and glued laminated timber with superior mechanical properties: Characterisation and application in strained gridshells. In: Construction and Building Materials 265, 25 pp.

5. BOCANEGRA, A.J.L., MAJANO, A., ORTIZ, J. & GUAITA, M. (2022): Structural Analysis and Form-Finding of Triaxial Elastic Timber Gridshells Considering Interlayer Slips: Numerical Modelling and Full-Scale Test. In: Applied science 12 (11), 26 pp.
6. CICHOCKA, J.M. (2020): Design and construction of a sequentially erected elastic timber gridshell. Massachusetts Institute of Technology. Thesis. 92 pp.
7. COLLABELA, S., LANCIA, D., REPOLA, L. & MEMMOLO, R. & PONE, S. (2015): A monitoring system for wooden post-formed gridshells. In: Conference IASS, 13 pp.
8. COLLINS, M. (2016): A computational and experimental study of Irish orientated strand board in bending active gridshells. University of Limerick. Thesis.
9. COLLINS, M., O´REGAN, B., COSGROVE, T. (2015): Potential of Irish Orientated Strand Board in Bending Active Gridshells. In: International Conference on Civil, Structural and Environmental Engineering, 9 pp.
10. CUVILLIERS, P. (2020): The constrained geometry of structures: Optimization methods for inverse form-finding design. Massachusetts Institute of Technology. Thesis. 145 pp.
11. DOUGLAS, C.M., PECK, E.A. & VINING, G.G. (2012): Introduction to Linear regression Analysis. John Wiley & Sons Inc. ISBN 978-0470542811. 872 pp.
12. D´AMICO, B. (2015): Timber Grid-shell Structures: form-finding, analysis and optimization. Doctor of Philosophy thesis. Edinburg Napier University. 161 pp.
13. D´AMICO, B. & ZHANG, H. (2014): A FORM FINDING METHOD FOR POST FORMED TIMBER GRID SHELL STRUCTURES. In: World Conference Timber Engineering, 7 pp.
14. D´AMICO, B., KERMANI, A., ZHANG, H. (2016): Form finding and structural analysis of actively bent timber grid shells. In: Engineering Structures 81, 195-207 pp.
15. EN 408, 2005: Timber structures. Structural timber and glued laminated timber. Determination of some physical and mechanical properties.
16. GENGNAGEL, CH., ALPERMANN, H., HERNÁNDEZ, E.L. (2014): Active bending in Hybrid Structures. In: Innsbruck university press. 18 pp.
17. GENGNAGEL, CH., HERNÁNDEZ, E.L., BÄUMER, R. (2013): Natural-fibre-reinforced plastic in actively bent structures. In: Construction Materials 166 (6), 365-377pp.
18. LIENHARD, J., GENGNAGEL, CH., KNIPPERS, J., ALPERMANN, H. (2013): Active bending. A review on structures where bending is used as a self-formation process. In: International Journal of Space Structures 28 (2-3), 187-196 pp.
19. LIDDEL, I. (2015): Frei Otto and the development of gridshells. In: Case Studies in Structural Engineering, Volume 4, 39-49pp.
20. MESNIL, R. (2013): Stability of elastic gridshells. Massachusetts Institute of Technology. Thesis. 115 pp.
21. PURBA, C.Y.C. (2019): Characterization and valorization of secondary quality hardwood as structural material. Vegetal Biology. AgroParisTech, NNT: 2019GPT0002, 150 pp.
22. QUINN, G. (2018): Pneumatic erection of elastic gridshells. Design, simulation & realization. Universität der Künste Berlon. Thesis. 205 pp.

23. QUINN, G., WILLIAMS, Ch. J., GENGNAGEL, CH. (2015): Comparison of erection methods for long-span strained grid shells. Conference: International Association for Shell and Spatial Structures (IASS). 13pp.
24. RAVENSHORST, G.J.P., VRIES, P.A., KUILEN, J.W. (2014): Aspects of the difference between the local and global modulus of elasticity of structural (hardwood) timber. In: Materials and Joints in Timber Structures, Conference paper, 773-783 pp.
25. ZEMIAR, J. (2007): Secondary technology wood processing. Part I.: Technology of furniture production. Department of distance education. Faculty of woodworking. Technical university of Zvolen. 144 pp.

ROMAN HERDA*, MILOŠ SLIVANSKÝ, JÁN BRODNIANSKY, TOMÁŠ KLAS
SLOVAK UNIVERSITY OF TECHNOLOGY IN BRATISLAVA
DEPARTMENT OF STEEL AND TIMBER STRUCTURES
RADLINSKÉHO 2766/11, 810 05
BRATISLAVA, SLOVAKIA
*Corresponding author: roman.herda@stuba.sk